THE JOURNAL OF PHYSICAL CHEMISTRY A

Article

Cite This: J. Phys. Chem. A 2017, 121, 9045-9057

pubs.acs.org/JPCA

Luminescence of Molecular Nitrogen Nanoclusters Containing Stabilized Atoms

Published as part of The Journal of Physical Chemistry virtual special issue "W. Lester S. Andrews Festschrift".

Patrick T. McColgan,[†] Adil Meraki,[‡] Roman E. Boltnev,[¶,§] David M. Lee,[†] and Vladimir V. Khmelenko*[,†]

[†]Department of Physics and Astronomy and Institute for Quantum Science & Engineering, Texas A&M University, College Station, Texas 77843, United States

[‡]Department of Physics, Bilecik University, 11210 Gülümbe, Bilecik, Turkey

[¶]Talrose Institute for Energy Problems of Chemical Physics, Russian Academy of Sciences, Chernogolovka, Russia

[§]Joint Institute for High Temperatures, Russian Academy of Sciences, Moscow, Russia

ABSTRACT: We studied the luminescence of molecular nitrogen nanoclusters containing stabilized nitrogen, oxygen, hydrogen, and deuterium atoms. Optical spectra were observed during the destruction of these ensembles of nanoclusters accompanied by a rapid release of chemical energy stored in the samples. Several interesting features were observed including a broad band near $\lambda \approx 360$ nm, which was identified as emission corresponding to $2A_g \rightarrow 1A_g$ transition of $N_4(D_{2h})$ polymeric nitrogen. Also the sharp lines at $\lambda \sim 336$ and 473 nm were observed, and their assignments to ND radicals are discussed.

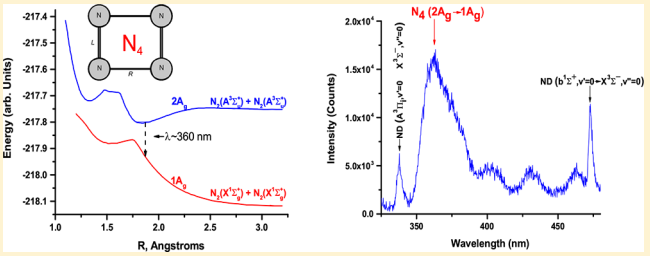

INTRODUCTION

Chemical and physical processes occurring in solid nitrogen have stimulated a broad range of research including studies of ices present in the interstellar medium,[1] as well as studies of high-energy density materials (HEDM). A promising method in the search for high-energy density systems has achieved local concentrations as high as 2×10^{21} cm^{-3} of stabilized nitrogen atoms in aerogel-like ensembles of nitrogen nanoclusters submerged in superfluid helium.[2−5] In this method the products of a radio frequency (RF) discharge in nitrogen−helium gas mixtures were injected into bulk superfluid helium, resulting in the production of ensembles of molecular nitrogen nanoclusters containing very high concentrations of stabilized nitrogen atoms.[6,7] This method also holds promise for the study of low-temperature chemical reactions in ensembles of nanoclusters. For example, exchange tunneling reactions between atoms and molecules of hydrogen isotopes were studied in nanoclusters immersed in superfluid helium.[8−11] Another possibility is the investigation of chemical reactions of a variety of heavier atoms and molecules during the warming of ensembles of nanoclusters containing stabilized atoms. Earlier investigations of chemical reactions during warming were performed in ensembles of molecular nitrogen and nitrogen−rare gas nanoclusters containing stabilized N and O atoms.[12−15] Rapid release of stored chemical energy in the samples resulted in intense thermoluminescence. In the optical spectra of thermoluminescence the bands of N and O atoms as well as N_2, NO, and O_2 molecules were observed. During investigations of the dynamics of spectra accompanying the destruction of these samples, it was found that during the process of annealing by raising the sample temperature, the emission of N and O atoms and the Vegard−Kaplan (V-K) bands of N_2 molecule were present. At the end of the destruction process bright flashes were observed, and in the spectra of these flashes, intense bands of O atoms and NO and O_2 molecules were present.[16] It was found that small changes in the oxygen content in the nanoclusters drastically influenced the optical spectra obtained.[16] This earlier work provided examples of observations of chemical reactions in collections of nanoclusters containing stabilized nitrogen and oxygen atoms.

In the experiment presented in this work, we added hydrogen or deuterium molecules into the gas mixtures used for preparing the samples in bulk superfluid helium. First, we expected that the addition of a small quantity of hydrogen isotopes would increase the efficiency of dissociation of atoms in the radio-frequency (RF) discharge zone, creating samples with the highest energy content.[17] During destruction of these samples, new nitrogen compounds such as polynitrogen molecules might be formed. The synthesis of HEDMs is a significant problem, and a promising direction is to synthesize polymeric nitrogen. A large energetic release from polynitrogen molecule decomposition provides a strong motivation to study

Received: September 28, 2017
Revised: November 3, 2017
Published: November 7, 2017

DOI: 10.1021/acs.jpca.7b09661
J. Phys. Chem. A 2017, 121, 9045−9057

polynitrogen as a clean HEDM. Such materials decompose into environmentally clean N_2 and produce enormous amounts of energy per unit mass without harmful waste.[18] Theoretical calculations have evaluated the structure and stability of numerous isomers of possible N_n molecules with n ranging from 3 to 60, but only some of the isomers are good candidates for HEDM. Neutral and ionic species N_3, N_3^+, N_3^-, N_4^+, were detected and studied in solid nitrogen films.[19−24] A cation N_5^+ has been synthesized as a part of a compound.[25,26] There are some detailed reviews of experimental and theoretical work on polynitrogen compounds in the literature.[27,28] Experimental evidence was obtained for the existence of tetranitrogen (tetrazete), N_4, in the gas and solid phases.[29−32] Matrix-isolated tetranitrogen was obtained by condensing products of an electrical discharge on a cold window,[31] or by bombarding solid nitrogen by electrons.[32] In the later case an intense broad band at λ = 360 nm was observed, which was assigned to the emission of $N_4(D_{2h})$ tetranitrogen. There are several approaches for the creating the N_4 species. The formation of N_4^+ cations followed by a neutralization reaction with electrons has been experimentally realized.[29−32] However, the association of two metastable $N_2(A^3\Sigma_u^+)$ molecules was suggested as an alternative mechanism for the formation of N_4 polynitrogen.[33] The conditions during our experiments are ideal for testing this suggestion. In our experiments, molecular nitrogen nanoclusters with high concentrations of stabilized $N(^4S)$ atoms were formed. During destruction of the ensembles of nanoclusters, $N(^4S)$ atoms recombine and create a large quantity of metastable $N_2(A^3\Sigma_u^+)$ molecules. Interactions of pairs of these molecules during the explosive destruction of the samples can lead to the formation of N_4 polymers, which could be identified by the light emitted at λ = 360 nm.[32]

Second, the addition of hydrogen or deuterium in the nitrogen−helium gas mixture provides the possibility of observing radicals containing H or D atoms such as the NH (ND) radicals. Eight emission systems of the NH radical have been found in the range from vacuum UV at 160 nm to near IR at ∼1.2 μm.[34,35] The most intense transition is the triplet system $A^3\Pi \rightarrow X^3\Sigma^-$ with a maximum around 336 nm. This band is a chief characteristic of the NH radical.[17,36−43] The singlet systems $c^1\Pi \rightarrow a^1\Delta$ at λ = 324 nm,[44,45] $c^1\Pi \rightarrow b^1\Sigma^+$ at λ = 450 nm,[46,47] and $d^1\Sigma^+ \rightarrow b^1\Sigma^+$ at λ = 162 nm[34,48] have been observed in gas-phase spectra. The weak, forbidden transitions $a^1\Delta \rightarrow X^3\Sigma^-$ at λ = 795 nm[35,49] and $b^1\Sigma^+ \rightarrow X^3\Sigma^-$ at λ = 471 nm[35,50] were observed in the emission spectra of NH (ND) in noble-gas matrices. Recently, the transition between the two lowest metastable states $b^1\Sigma^+ \rightarrow a^1\Delta$ was detected at 1.17 μm in the emission spectra of matrix-isolated NH.[35] In our experiments, the spectra were thoroughly examined in these spectral regions to observe the bands of NH (ND) radicals.

In this work we mainly studied the dynamics of optical spectra during the destruction of ensembles of molecular nitrogen nanoclusters containing stabilized nitrogen, oxygen, and also hydrogen or deuterium atoms. We found that in the spectra of the samples prepared from deuterium−nitrogen−helium gas mixtures the bands at λ = 336, 360, and 471 nm are present in addition to bands observed during destruction of nanoclusters containing only N and O atoms. The intensity of all bands in the spectra were influenced by the presence of admixtures of hydrogen isotopes. We conclude that the band at λ = 360 nm belongs to the emission of the N_4 compound, supporting the results obtained in ref 32. Possible mechanisms for the formation of the N_4 compounds are discussed. The emission at λ = 336 nm was assigned to the $A^3\Pi$, $v' = 0 \rightarrow X^3\Sigma^-, v'' = 0$ transition of ND radicals. The assignment of 473 nm band is still controversial. Two species, namely, ND radicals and N^- anions,[51] may be responsible for this emission.

EXPERIMENTAL SETUP

Our experimental setup has been described elsewhere.[16] The cryogenic portion of the experimental setup consists of two silvered-glass double-walled Dewars. The outer Dewar is filled with liquid nitrogen (LN_2), and the inner Dewar is filled with liquid helium (LHe). This inner Dewar is pumped by an Edwards model E2M80 rotary pump. With this vacuum pump, temperatures of ∼1.1 K of the liquid helium bath are achievable.

Gas mixtures are prepared at room temperature using a gas handling system. This system consists of a manifold that connects storage tanks, mixing tanks, vacuum pumping lines, and a flux controller for supplying and controlling gas mixtures to the cryogenic system. In our experiments we used hydrogen−nitrogen−helium gas mixtures. Research-grade helium gas from Linde Electronics & Specialty Gases with 99.999% purity was used. The oxygen content in the gas mixtures resulted from contamination in this gas (∼1 ppm).

The samples are created by injecting a gas mixture through an RF discharge zone into superfluid helium (HeII).[6,7] The atomic source is made of a cylindrical outer quartz tube with a concentric inner quartz capillary. At the bottom of the tube there are two electrodes, which surround the capillary. The tube is filled with LN_2, which simultaneously cools the incoming gas mixture and the discharge electrodes. The ∼75 W RF discharge with frequency of ∼50 MHz is provided by an HP 8556B signal generator amplified by an E&I 3100L amplifier. The gas mixture exits the discharge zone through an orifice with diameter ∼0.75 mm, which is 2 cm above the level of HeII inside the beaker. A pressure gradient of ∼2 torr creates a well-formed gas jet that penetrates the surface of the HeII, where the gas mixture containing dissociated impurity atoms and excited species forms ensembles of nanoclusters. The level of HeII in the sample collection beaker was kept constant by filling with a thermomechanical fountain pump, which sent HeII from the bottom of the main bath. During sample preparation, the temperature of HeII was maintained at 1.5 K. The temperature inside of the beaker is measured by using a germanium thermometer.

After the sample accumulates for 10−30 min, the flow of gas mixture is ceased, and the RF discharge is turned off. The fountain pump is then turned off. Over the course of 20−30 min, the HeII exits the beaker by processes of evaporation and creeping film, leaving a dry sample. When the liquid helium is nearly removed from the beaker, the pumping line is closed allowing the temperature of the sample to increase from 1.2 to 15 K in ∼50 s and initiate destruction of the sample. Thermoluminescence from the sample increases with temperature, until the sample is completely destroyed. This process is accompanied by a series of bright flashes.

The optical spectra are obtained using a special bifurcated optical fiber assembly part of which was installed inside the helium Dewar, where it was able to withstand liquid-helium temperatures.[16] By employing this bifurcated fiber assembly, we could make simultaneous measurements in two different spectrometers, the Andor Shamrock SR-500i spectrometer with Newton EMCCD camera and the Ocean Optics HR2000+ spectrometer.

DOI: 10.1021/acs.jpca.7b09661
J. Phys. Chem. A 2017, 121, 9045−9057

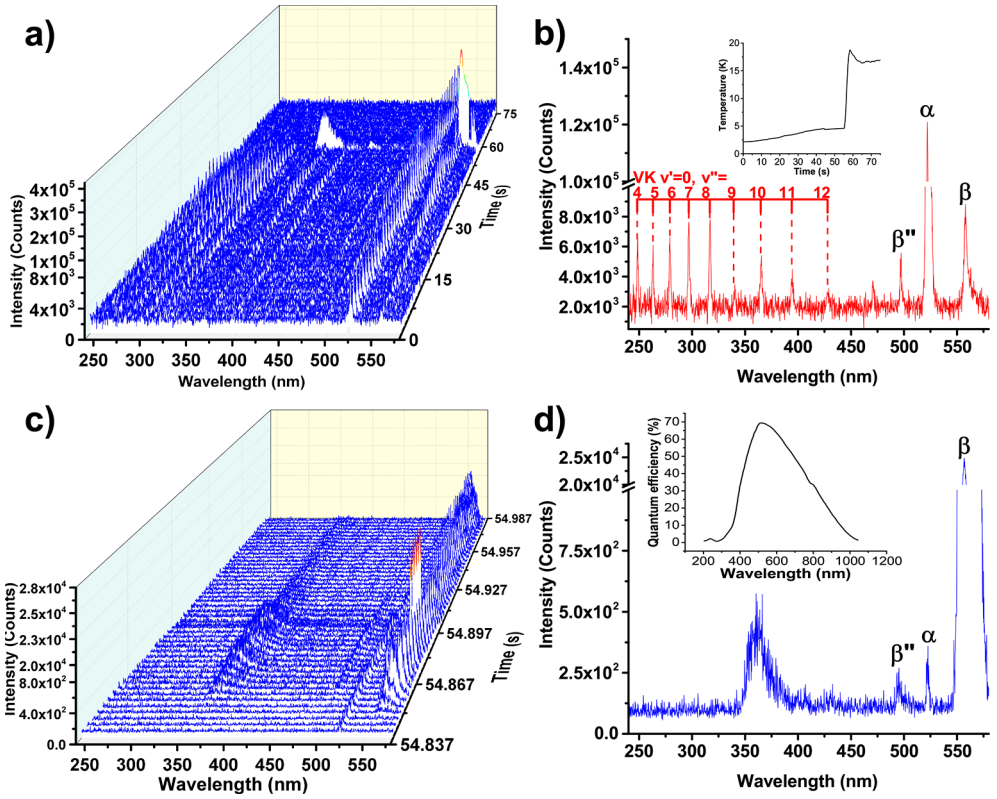

Figure 1. Spectra taken in the range of 240−580 nm by the Andor spectrometer during destruction of the sample prepared from gas mixture $[H_2]/[N_2]/[He]$ 1:330:33 000. (a) Dynamics of luminescence spectra for the entire destruction process. Each spectrum was accumulated during a period of 1.5 s. (b) Spectrum taken during destruction at t = 37.5 s with band identifications. (inset) Temperature dependence on time during sample destruction. (c) Dynamics of luminescence spectra during the final period of destruction (150 ms) of the sample with exposure time of 3 ms. (d) Spectrum taken at the end of sample destruction corresponds to t = 54.891 s with band identifications. (inset) Quantum efficiency of the Andor spectrometer.

The high-sensitivity Andor spectrometer can take high-resolution spectra (0.53 nm, first grating) and can capture spectra with an exposure time of 3 ms in a limited ($\Delta\lambda \approx 340$ nm) spectral range. The Ocean Optics spectrometer can take spectra over a large wavelength range (from 200 to 1100 nm) with the resolution of 1.3 nm and generally uses an exposure time varying from 100 to 300 ms.

EXPERIMENTAL RESULTS

Influence of Hydrogen on Thermoluminescence Spectra of Ensembles of Nitrogen Nanoclusters. First we studied the destruction process of samples prepared from the gas mixture $H_2/N_2/He$ = 1:330:33 000. Figures 1 and 2 show the dynamics of luminescence during the destruction of samples prepared from gas mixture $H_2/N_2/He$ = 1:330:33 000 in the wavelength range from 240 to 580 nm and 540−880 nm, respectively. Figure 1a shows the dynamics of the emission of α-group of N atoms, V-K bands of N_2 molecules, and β- and β''-groups of O atoms,[16] which were observed from the beginning of sample thermoluminescence. The intensities of these features increase with temperature. The spectrum of emission observed during the early stage of destruction, with identification of bands, is shown in Figure 1b. At the end of the destruction during bright flashes, the intense β-group and the band with maximum at λ = 360 nm were most intense. The dynamics of thermoluminescence at the final stage destruction is shown in Figure 1c. During the time period of 60 ms the correlation between the emission of the β-group and the band with a maximum at λ = 360 nm were observed. The spectrum of the most intense flash with identification of the bands is presented in Figure 1d. The weak α-group of nitrogen atoms and β''-group of oxygen atoms are also present in this spectrum.

Figure 2a shows the dynamics of the emission of the β-group of O atoms, α'- and δ''-groups of N atoms, and the γ-line of N^- anions.[51] The intensity of all lines increased with temperature. The spectrum of the emission at the beginning of the destruction with the identification of all observed bands is shown in Figure 2b. The dynamics of the thermoluminescence during the last 900 ms of sample destruction is shown in Figure 2c with better time resolution. At the end of the destruction, the intense β-group of O atoms and γ-line of N^- anions, as well as weaker δ''-group of N atoms, and β'-group of O atoms were observed. The spectrum with identified bands corresponding to largest flashes at the end of destruction is shown in Figure 2d. The most striking change in the spectra compared to those obtained for nitrogen−helium samples[13,14,16] was the appearance of a broad band with maximum at λ = 360 nm. The positions and origins of the atomic and molecular bands in the spectra presented in Figures 1 and 2 are listed in columns 2 of Tables 1 and 3−5. The presence of α'-, β'-, β''-, and δ'-groups of N and O atoms in the spectra indicates that N_2 molecules are neighbors of these atoms.[16,52]

As a next step, we observed the influence of the presence of molecular hydrogen in the initial gas mixtures on the appearance of the band at λ = 360 nm. Thus, spectra were studied during destruction of the samples prepared from

DOI: 10.1021/acs.jpca.7b09661
J. Phys. Chem. A 2017, 121, 9045−9057

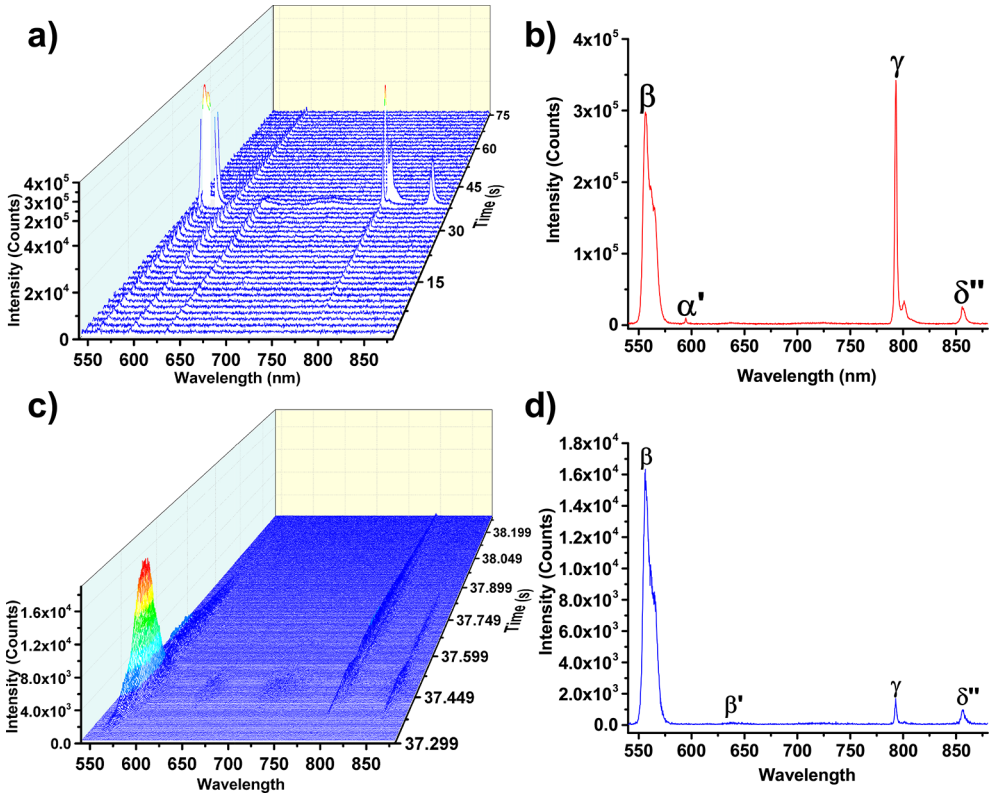

Figure 2. Spectra taken in the range of 540−880 nm with the Andor spectrometer during destruction of the sample prepared from gas mixture $[H_2]/[N_2]/[He]$ = 1:330:33 000. (a) Dynamics of the luminescence spectra during the entire destruction process. Each spectrum has an exposure time of 1.5 s. (b) Spectrum taken during destruction at t = 37.5 s with identification of all bands observed with exposure time of 1.5 s. (c) Dynamics of the luminescence spectra during the final period of sample destruction with exposure time of 3 ms. (d) Spectrum taken at the end of sample destruction at t = 37.491 s with band identifications.

Table 1. Positions (nm) of the V-K Bands $N_2(A^3\Sigma_u^+\ v' = 0 \rightarrow X^1\Sigma_g\ v'')$ Observed during the Destruction of Samples Prepared from Different Gas Mixtures

band v′,v″	in N_2 matrix[53]	$[H_2]/[N_2]/[He]$ 1:330:33 000	$[D_2]/[N_2]/[He]$ 1:2000:100 000	$[D_2]/[N_2]/[Ar]/[He]$ 1:500:4500:225 000	$[D_2]/[N_2]/[Ne]/[He]$ 1:500:5000:100 000
0,4	248.4	248.6	250.08	248.2	248.9
0,5	263.0	263.2	263.22	263	263.7
0,6	278.9	279.1	278.69	278.6	279.5
0,7	296.8	296.8	296.49	296.4	297.1
0,8	316.8	317.2	318.12	315.9	317.2
0,9	339.3		337.9	338.3	340.1
0,10	365.2	365.5	365.65		365.5
0,11	393.5	394.4	394.3	394.9	394.6
0,12	427.1		429.99		

different H_2/N_2/He gas mixtures. The ratio between H_2/N_2 in these mixtures was changed from 1/200 to 1/500.

Figure 3 shows the integrated spectra of the emission observed with the Ocean Optics spectrometer during the destruction of samples prepared from different H_2/N_2/He gas mixtures. Lines and bands observed include the α-group and α'-group of N atoms, the γ-line of N^- anions, the V-K bands of N_2 molecules (v' = 0, v'' = 2−12), and the β-group of O atoms. This figure demonstrates the influence of the concentration of H_2 in the sample gas mixture on the intensity of the observed lines in the spectra. The integrals of intensities of bands shown in Figures 3 and 4 are listed in Table 2. The maximum intensities of the lines were observed for the gas mixture with the ratio of H_2/N_2 = 1/330 as shown in Table 2. The intensities of bands from the sample prepared from gas mixture with H_2/N_2 ratio equal to 1/200 are 4−9 times smaller, and the intensities of the bands of the sample prepared from gas mixture with ratio H_2/N_2 = 1/500 were twice smaller.

Figure 4 shows spectra of the emission of the largest flashes observed with the Ocean Optics spectrometer accompanying the destruction of samples prepared from gas mixtures with different H_2/N_2/He ratios. Lines and bands observed include the α-, δ-, and δ''-groups of N atoms, the γ-line of N^- anions,[51] the V-K bands of N_2 molecules, the β-group of O atoms, and the M-bands of the NO molecule. It is also interesting to note that for all samples made from gas mixtures with small admixtures of molecular hydrogen the broad feature at λ = 360 nm was clearly observed only in the spectra of the largest flashes. This figure demonstrates the same tendency between the concentration of H_2 in the gas mixture used for sample

DOI: 10.1021/acs.jpca.7b09661
J. Phys. Chem. A 2017, 121, 9045−9057

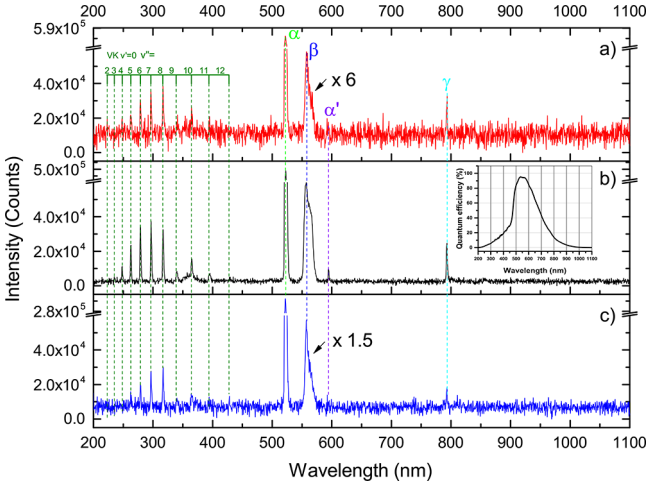

Figure 3. Integrated spectra observed with the Ocean Optics spectrometer during the entire destruction process for samples created from different $H_2/N_2/He$ gas mixtures: (a) $[H_2]/[N_2]/[He]$ = 1:200:20 000. (b) $[H_2]/[N_2]/[He]$ = 1:330:33 000. (inset) The quantum efficiency of the Ocean Optics spectrometer. (c)$[H_2]/[N_2]/[He]$ = 1:500:50 000.

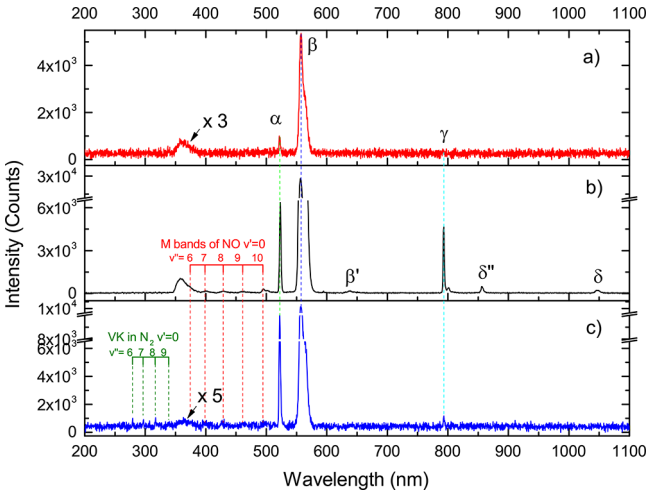

Figure 4. Spectra of the largest flashes during the destruction of samples formed by different hydrogen−nitrogen−helium gas mixtures: (a) $[H_2]/[N_2]/[He]$ = 1:200:20 000, (b) $[H_2]/[N_2]/[He]$ = 1:330:33 000, and (c) $[H_2]/[N_2]/[He]$ = 1:500:50 000. Spectra were taken with the Ocean Optics spectrometer with exposure time of 500 ms.

preparation and the intensity of the lines in the emitted spectra as was demonstrated in Figure 3. The most intense luminescence was observed for the sample prepared from the gas mixture with ratio of $H_2/N_2 \approx 1/330$ as shown in Table 2 and Figure 4. In contrast to the integrated spectra, in the spectra of the largest flashes, V-K bands are substantially suppressed, but a new rather intense band with maximum at λ = 360 nm appears. The intensity of the band at λ = 360 nm for gas mixture with H_2/N_2 ratio of 1/330 was 3 times greater than for the gas mixture with H_2/N_2 ratio of 1/200 and 4 times greater than for gas mixture with H_2/N_2 ratio of 1/500.

Influence of Deuterium on Thermoluminescence Spectra of Ensembles of Nitrogen Nanoclusters. To understand the origin of the band at λ = 360 nm we performed experiments to study the influence of the addition of D_2 molecules to N_2−He gas mixtures used for sample preparation on the spectra obtained during sample destruction. The isotope shift effect can help in the identification of bands corresponding to species containing hydrogen isotopes.

Figure 5a shows the dynamics of the emission of the α-group of N atoms, the V-K bands of N_2 molecules, and the β-group of O atoms, which were observed in the thermoluminescence of the sample prepared from the gas mixture $D_2/N_2/He$ = 1:2000:100 000. The intensities of the bands mentioned above increase with temperature. The spectrum of the emission is shown in Figure 5b near the end of destruction, where the emission from the V-K band is most intense. This spectrum also includes the strong α-group of N atoms, and the β-group of O atoms as well as other weaker lines including the β''-group from oxygen, and the line at λ = 473 nm. The dynamics of thermoluminescence at the end of destruction is shown in Figure 5c. During the time period of 60 ms, the intensity of emission of the β-group correlates with the intensity of the band at λ = 360 nm. The spectrum of this emission is shown in Figure 5d. The strong β-group of O atoms and the band at λ = 360 nm along with the weaker α-group of N atoms, and bands at 337 and 473 nm, are also present in this spectrum. The positions and origins of atomic and molecular bands in the spectra presented in Figure 5 are listed in column 3 in Tables 1 and 3−5. It is interesting to note that the appearance of the bands at λ = 336 nm and at λ = 473 nm in the samples prepared with addition of D_2 molecules is in contrast with the case of hydrogen-containing samples, where these bands were not observed.

We also studied the influence of the concentration of D_2 molecules in the N_2/He gas mixture used for sample preparation on the intensity of the bands in the spectra obtained during the destruction of the samples. Figure 6 shows the integrated spectra of the emission observed with the Ocean Optics spectrometer during the destruction of different D_2/N_2/He samples. Lines and bands observed include the α- and α'-groups of N atoms, the γ-line of N^- anions, the V-K bands of

Table 2. Integrals of the Intensities of Bands (arb. units) Observed during the Entire Destruction Process (Int) and during the Largest Flash (Flash) for Samples Prepared from Different Hydrogen−Nitrogen−Helium Gas Mixtures

	$[H_2]/[N_2]/[He]$		$[H_2]/[N_2]/[He]$		$[H_2]/[N_2]/[He]$	
	1:200:20 000		1:330:33 000		1:500:50 000	
band	Int	Flash	Int	Flash	Int	Flash
α	1.92×10^5	1.73×10^3	1.74×10^6	2.06×10^4	9.02×10^5	6.62×10^3
β	1.41×10^5	2.10×10^4	9.03×10^5	3.44×10^5	4.73×10^5	3.01×10^4
γ	1.13×10^5	4.01×10^3	4.38×10^5	7.53×10^4	2.82×10^5	5.42×10^3
λ = 360 nm		5.49×10^4		1.75×10^5		4.06×10^4
VK (v′ = 0,v″ = 7)	3.39×10^5	9.76×10^3	1.62×10^6	6.00×10^3	1.00×10^6	1.22×10^4

DOI: 10.1021/acs.jpca.7b09661
J. Phys. Chem. A 2017, 121, 9045−9057

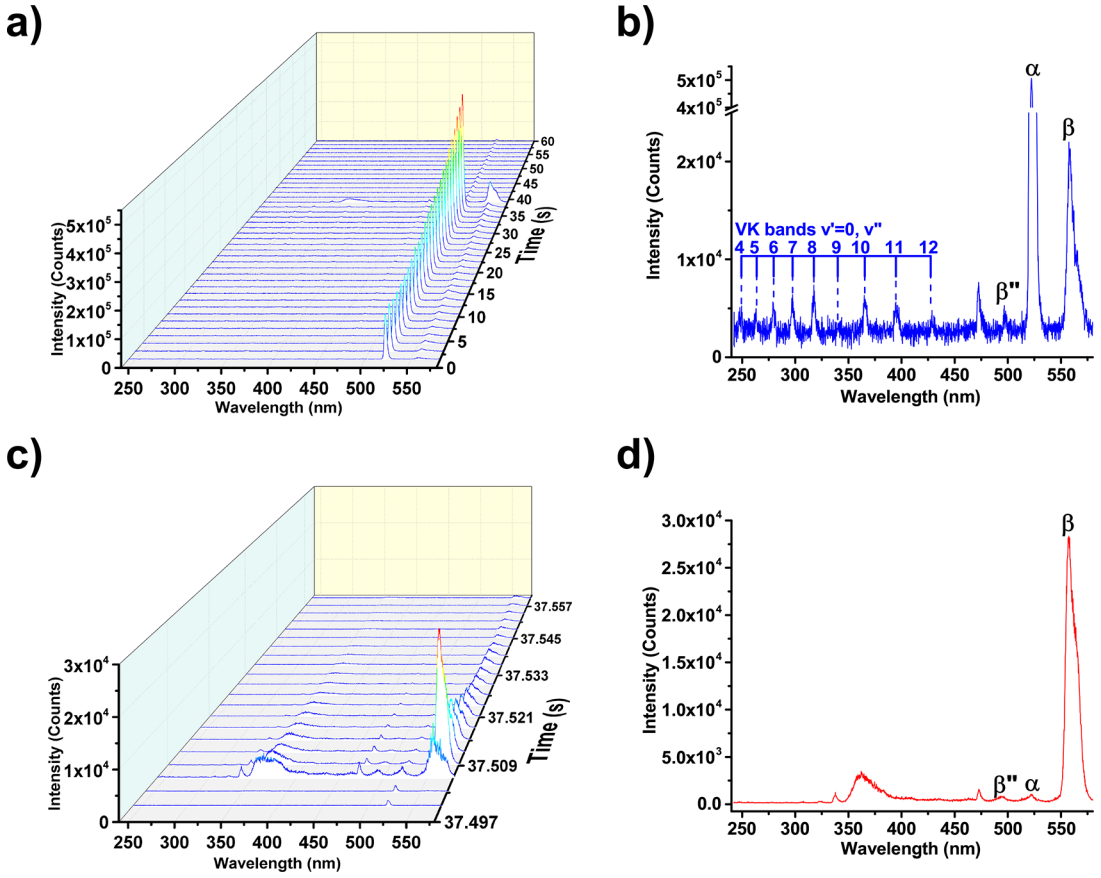

Figure 5. Spectra taken in the range of 240−580 nm with the Andor spectrometer. Spectra were observed during the destruction of the sample prepared from gas mixture $[D_2]/[N_2]/[He]$ = 1:2000:100 000: (a) Luminescence dynamics for the entire destruction process. Each spectrum has an exposure time of 1.5 s. (b) Spectrum taken at t = 34.5 s with 1.5 s exposure time with band identifications. (c) Dynamics during the final stage (60 ms) of the sample destruction. Each spectrum has exposure time of 3 ms. (d) Spectrum taken at the end of destruction at t = 37.509 s with 3 ms exposure time with band identifications.

Table 3. Positions (nm) of Lines of N and O Atoms, and Nitrogen Anion Observed during the Destruction of Samples Prepared from Different Gas Mixtures

	in N_2 matrix[54]	$[H_2]/[N_2]/[He]$ 1:300:30 000	$[D_2]/[N_2]/[He]$ 1:2000:100 000	$[D_2]/[N_2]/[Ar]/[He]$ 1:500:4500:225 000	$[D_2]/[N_2]/[Ne]/[He]$ 1:500:5000:100 000
α	522.8	522	522.3	523.7	523.3
α'	594.4	594.5		592.1	594.5
δ''	857				857.2
β	554.9	557.8	557.4	559.1	557.6
β'	636.7	633.2		632.7	
β''	494				
γ	791	793	794.0	794.2	793.8

Table 4. Positions (nm) of "New" Lines Emitted during the Destruction of Samples Prepared from Different Gas Mixtures with the Addition of Hydrogen and Deuterium Molecules

in N_2 matrix	$[H_2]/[N_2]/[He]$ 1:330:33 000	$[D_2]/[N_2]/[He]$ 1:2000:100 000	$[D_2]/[N_2]/[Ar]/[He]$ 1:500:4500:225 000	$[D_2]/[N_2]/[Ne]/[He]$ 1:500:5000:100 000
336 (ND)[41]		337.8	336.6	337.7
471 (ND)[41]		472.9	473.9	472.4
360 (N_4^+)[32]	361.9	363.3	361.5	365.1

N_2 molecules ($v' = 0$, $v'' = 2$−13), and the β-group of O atoms. This graph demonstrates that there exists an optimal concentration of D_2 in the gas mixture used for sample preparation that produces a maximum intensity for all lines of luminescence during sample destruction. This optimum concentration of D_2 corresponds to the spectra shown in Figure 6b. The integrals of intensities of the bands shown in Figures 6 and 7 are listed in Table 6.

Figure 7 shows spectra of the emission observed with the Ocean Optics spectrometer for the largest flashes during

DOI: 10.1021/acs.jpca.7b09661
J. Phys. Chem. A 2017, 121, 9045−9057

Table 5. Positions (nm) of NO−M Bands ($a^4\Pi$, v′ = 0→$X^2\Pi$, v″) and NO β-Bands ($B^2\Pi$, v′ = 0→$X^2\Pi$, v″) Observed during the Destruction of Samples Prepared from Different Gas Mixtures

	N_2	$[H_2]/[^{14}N_2]/[He]$	$[D_2]/[N_2]/[He]$	$[D_2]/[N_2]/[Ar]/[He]$	$[D_2]/[N_2]/[Ne]/[He]$
v′,v″	matrix[55]	1:300:30 000	1:2000:100 000	1:500:4500:225 000	1:500:5000:100 000
NO−M bands					
0,7	399.41	394.8	398.8	401.6	395.2
0,8	428.71	429.0	429.4	430.9	429.9
0,9	462.00	464.1	463.6		
0,10	494.4[16]	496.8	494.2	494.6	496.6
NO-β bands					
0,8	322.40	323.5			324.4
0,9	340.40	340.7			339.4
0,10	359.30				
0,11	383.75[16]	384.0			384.0

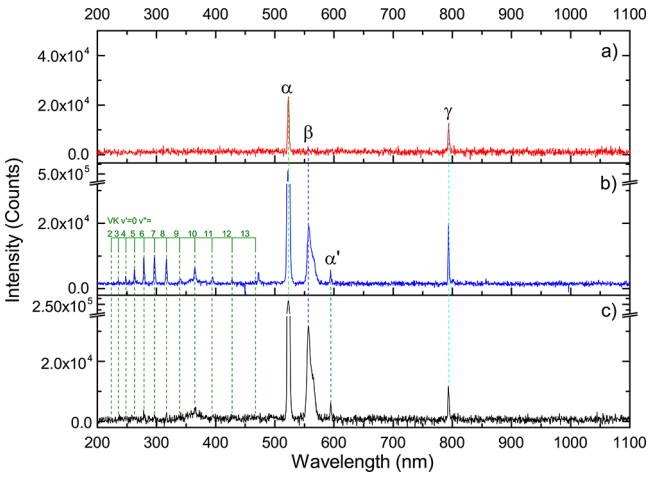

Figure 6. Integrated spectra taken with the Ocean Optics spectrometer during the destruction of samples created from different deuterium−nitrogen−helium gas mixtures: (a) $[D_2]/[N_2]/[He]$ = 1:750:50 000, (b) $[D_2]/[N_2]/[He]$ = 1:2000:100 000, and (c) $[D_2]/[N_2]/[He]$ = 1:10 000:500 000.

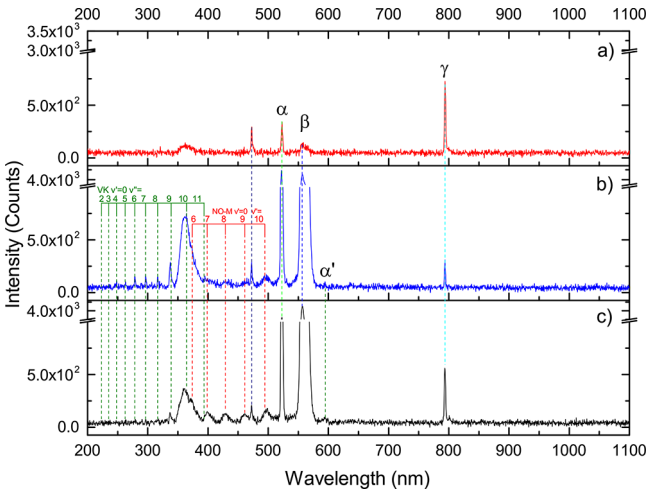

Figure 7. Spectra taken with the Ocean Optics spectrometer of the largest flashes during the destruction of samples created from different deuterium−nitrogen−helium gas mixtures: (a) $[D_2]/[N_2]/[He]$ = 1:750:50 000, (b) $[D_2]/[N_2]/[He]$ = 1:2000:100 000, (c) $[D_2]/[N_2]/[He]$ = 1:10 000:500 000.

destruction of samples prepared from different $D_2/N_2/He$ gas mixtures. Lines and bands observed include the broad band at λ = 360 nm, the α-group of N atoms, the γ-line of N^- anions, the weak V-K bands of N_2 molecules (v′ = 0, v″ = 2−11), the strong β-group of O atoms, and the M-bands of NO molecules (v′ = 0, v″ = 6−10). This graph demonstrates the similar relation between the concentration of D_2 in the gas mixture used for sample preparation and the intensity of the luminescence observed during sample destruction as was shown in Figure 6. The optimum concentration of D_2 for observation of the most intense bands corresponds to the $[D_2]/[N_2]/[He]$ = 1:2000:100 000 gas mixture as can be seen from Table 6. The spectrum of the sample created from this gas mixture is shown in Figure 7b. It is also interesting to note that in all spectra of the largest flashes of the samples prepared from $D_2/N_2/He$ gas mixtures, the intense broad feature at λ = 360 nm was observed.

Destruction of Samples Prepared from Argon- and Neon-Containing Mixtures. To observe possible matrix effects on the positions of the atomic and molecular bands, we also studied samples prepared from deuterium−nitrogen−helium gas mixtures with the addition of rare gases Ne and Ar.

Figure 8a shows the dynamics of the emission of the sample prepared from gas mixture $D_2/N_2/Ar/He$ = 1:500:4500:225 000. The α-group of N atoms, the V-K bands of N_2 molecules, and the β-group of O atoms were observed from the beginning of sample thermoluminescence. The intensities of these features increase with temperature. The spectrum of the sample emission with identification of bands is shown in Figure 8b. The spectrum was observed near the end of destruction, where the emission from the VK band is most intense. This spectrum also includes the strong α-group of N atoms, the β-group of O atoms, and in addition other weaker lines at λ = 473 and the β''-group of oxygen. The dynamics of thermoluminescence during the brightest flashes is shown in Figure 8c. During the time period of 60 ms the emission of α-group, the β- and β''-groups and bands at λ = 336 nm and λ = 473 nm, as well as the broad feature at λ = 360 nm, were observed. The spectrum of this emission with band identifications is shown in Figure 8d.

Figure 9 shows a comparison of spectra taken during the destruction of samples created from deuterium−nitrogen−helium gas mixtures as well as those formed with the addition of rare gases Ne and Ar. Features observed in this spectra include the strong α-group of N atoms and the β-group of O atoms, the V-K bands of N_2 molecules (v′ = 0, v″ = 4−11), the M bands of NO molecules (v′ = 0, v″ = 6−10), along with the broad band with maximum at λ = 360 nm, and the bands at λ = 336 nm and at λ = 473 nm. The most intense flash was from

DOI: 10.1021/acs.jpca.7b09661
J. Phys. Chem. A 2017, 121, 9045−9057

Table 6. Integrals of the Intensities of Bands (arb. units) Observed during the Entire Destruction Process (Int) and during the Largest Flash (Flash) for Samples Prepared from Different Deuterium−Nitrogen−Helium Gas Mixtures

	$[D_2]/[N_2]/[He]$ 1:750:50 000		$[D_2]/[N_2]/[He]$ 1:2000:100 000		$[D_2]/[N_2]/[He]$ 1:10 000:500 000	
band	Int	Flash	Int	Flash	Int	Flash
α	8.47×10^4	1.41×10^3	1.58×10^6	1.76×10^4	1.16×10^6	1.19×10^4
β	4.12×10^4	2.58×10^3	2.41×10^5	5.81×10^4	3.58×10^5	5.05×10^4
γ	2.24×10^5	1.24×10^4	2.86×10^5	5.07×10^3	2.01×10^5	1.11×10^4
λ = 360 nm		2.58×10^4		1.25×10^5		6.77×10^4
V-K v′ = 0,v″ = 7	1.23×10^5	5.13×10^3	5.47×10^5	9.48×10^3	1.15×10^5	4.86×10^3

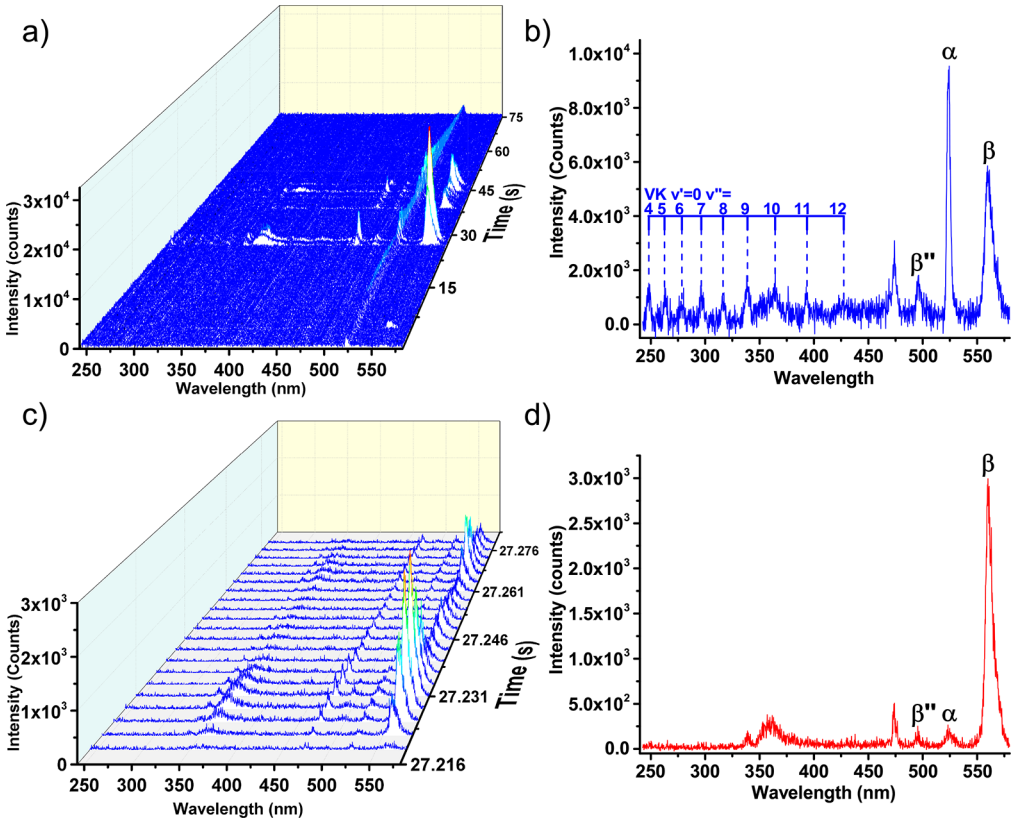

Figure 8. Spectra taken in the range of 240−580 nm with the Andor spectrometer. Spectra observed during the destruction of the sample prepared from gas mixture $[D_2]/[N_2]/[Ar]/[He]$ = 1:500:4500:225 000: (a) Dynamics of spectra during the entire destruction process with exposure time of 1.5 s. (b) Spectrum taken at t = 44.1 s with 1.5 s exposure time with identification of all observed bands. (c) Dynamics of spectra taken with exposure time of 3 ms during the final stages of the sample destruction. (d) Spectrum taken at t = 27.231 s with 3 ms exposure time with identification of observed bands.

the sample prepared from the gas mixture containing neon. The positions and origins of atomic and molecular bands in the spectra presented in Figures 5 and 9 are listed in columns 3−5 of Tables 1 and 3−5.

DISCUSSION

We have studied the destruction of nanostructures with high densities of stored chemical energy. The fast release of chemical energy resulted in intense sample thermoluminescence. The nanostructures were formed by nanoclusters of molecular nitrogen in bulk superfluid helium. The average size of these nanoclusters was ∼5 nm with an overall density of impurity material in liquid helium of order $\sim 1 \times 10^{20}$ cm^{-3} as determined form X-ray experiments.[56−61] Nanoclusters form porous aerogel-like structures with a wide distribution of pore sizes from 8 to 800 nm.[62,63] The pores initially were filled with liquid helium.[57] The stabilized atoms reside mostly on the surface of the nanoclusters.[5,64,65] The average concentration of stabilized nitrogen atoms was of order 1×10^{19} cm^{-3},[3,4] and the local concentrations of nitrogen atoms in the nanoclusters were of order 1×10^{21} cm^{-3} as determined by the width of electron spin resonance (ESR) spectra.[5] These samples contained O atoms and H(D) atoms, whose concentrations were from 1×10^3 to 1×10^4 times smaller than the N atom concentrations. As a result, the porous structures formed by molecular nitrogen nanoclusters containing stabilized atoms are characterized by high specific energy content (up to 1×10^4 J/g).[2,3] These structures were stable while immersed in bulk superfluid helium. Removing liquid helium from the structures led to a collapsing of the pores and the initiation of chemical reactions of atoms residing on the surfaces of the nanoclusters. At the beginning of the sample destruction we observed an increase of the emission of the sample. In the earlier work these structures were formed by nitrogen molecules and atoms with a small

DOI: 10.1021/acs.jpca.7b09661
J. Phys. Chem. A 2017, 121, 9045−9057

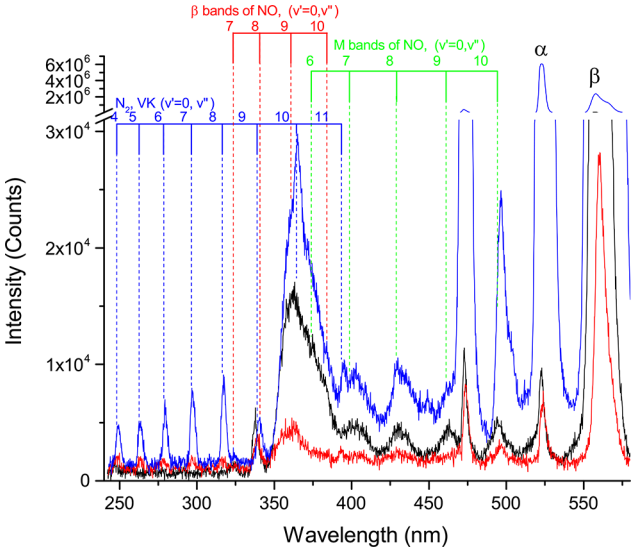

Figure 9. Spectra of the largest flash observed by the Andor spectrometer with resolution of 0.5 nm during the destruction of samples prepared from different gas mixtures: $[D_2]/[N_2]/[Ne]/[He]$ = 1:500:5000:100 000 (blue), $[D_2]/[N_2]/[Ar]/[He]$ = 1:500:4500:225 000 (red), and $[D_2]/[N_2]/[He]$ = 1:2000:100 000 (black).

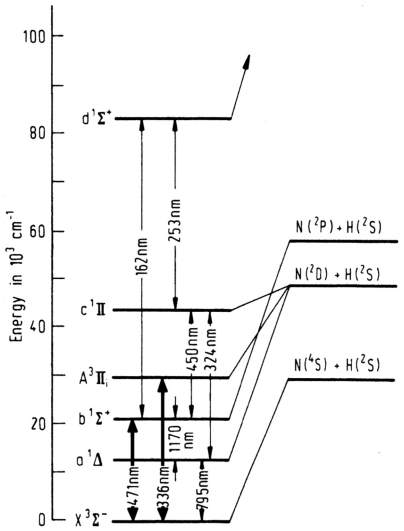

Figure 10. Energy diagram for NH radicals.[66] The transitions observed in this work are shown as thicker arrows.

admixture of O atoms ($N_2/O_2 \approx 1 \times 10^{-3}$ to 1×10^{-4}). This explains the spectra obtained during the destruction of the samples, where in addition to the expected α- and α'-bands of nitrogen atoms and the V-K bands of N_2 molecules, the β-,β'-,β''-bands of O atoms, M- and β-bands of NO molecules and even the second Herzberg bands of O_2 molecules were observed.[12−14,16] The addition of hydrogen or deuterium molecules into the gas mixtures used for sample preparation can lead to the appearance of luminescence from some new species formed in chemical reactions during the destruction of these samples. It was found that a relatively small change of the hydrogen and deuterium impurity content drastically influenced the spectra obtained (see Figures 3, 4, 6, and 7). Indeed, in the spectra obtained during the destruction of samples prepared from deuterium−nitrogen−helium gas mixtures we observed new intense bands at λ = 336, 360, and 473 nm and for samples prepared from hydrogen−nitrogen−helium gas mixtures we observed only one new intense band at λ = 360 nm in addition to the bands observed in the spectra obtained from samples prepared from "pure" nitrogen−helium gas mixtures.[14,16]

Possible candidates for emission of these bands may be species containing H and D atoms such as the radicals NH and ND. The energy levels and transitions of the NH radical are presented in Figure 10. The transitions $A^3\Pi_i \rightarrow X^3\Sigma^-$ and $b^1\Sigma^+ \rightarrow X^3\Sigma^-$ of ND can be responsible for emission at λ = 336 and 473 nm, respectively. The position of the ND bands in different matrices is shown in Table 7. The observed positions of the new lines at λ = 336 and 473 nm shown in Table 4 are close to the positions of ND radical lines in the rare-gas matrices (see Table 7). Assignment of emission at λ = 473 nm to the $b^1\Sigma^+$, v′ = 0→$X^3\Sigma^-$, v″ = 0 transition of the ND radicals are also supported by a decrease of the emission of δ- and δ''-groups of N atoms in the spectra when the band at λ = 473 nm is present (see Figure 7). The $b^1\Sigma^+$-state of ND radical is formed in the recombination of N(^{2}P) and D(^{2}S) atoms (see Figure 10). As a result of this reaction the N(^{2}P) atoms were removed from the system, and thus the δ- and δ''-emissions are

Table 7. Positions (nm) of NH and ND Transition $A^3\Pi_i$, v′ = 0→$X^3\Sigma^-$, v″ = 0 and $b^1\Sigma^+$, v′ = 0→$X^3\Sigma^-$, v″ = 0 in Different Rare-Gas Matrices[35,41]

radical	matrix	$A^3\Pi_i$, v′ = 0→$X^3\Sigma^-$, v″ = 0	$b^1\Sigma^+$, v′ = 0→$X^3\Sigma^-$, v″ = 0
NH	Ne	335.92[41]	
	Ar	337.76[41]	472.99[35]
	Kr	338.95[41]	
ND	Ne	335.57[41]	
	Ar	337.76[41]	473.26[35]
	Kr	338.73[41]	

absent. In the emission from hydrogen−nitrogen−helium samples the band at λ = 473 nm is absent, but the emission of the δ- and δ''-groups is present (see Figure 4), providing evidence that N(^{2}P) atoms have undergone radiative decay and thus did not participate in the reactions with H(^{2}S) atoms in this case.

An alternative interpretation for the line at λ = 473 nm may be the transition $^1S_0 \rightarrow {}^3P_1$ of N^- anion.[51] Figure 11 shows the

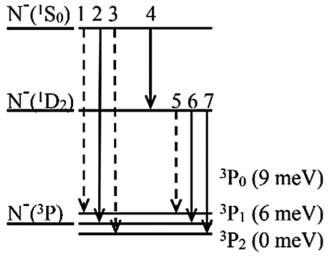

Figure 11. Energy diagram for N^- anions.[51]

energy diagram for the three lowest energy levels of the N^- anion. If the line at λ = 473 nm belongs to the $N^-(^1S_0 \rightarrow {}^3P_1)$ transition we can calculate the line corresponding to the $N^-(^1S_0 \rightarrow {}^1D_2)$ transition, because we know the position of the line corresponding to the $N^-(^1D_2 \rightarrow {}^3P_{1,2})$ transition (γ-line).[51] The position of the $N^-(^1S_0 \rightarrow {}^3D_2)$ transition should be at λ = 1167 nm. The position of this line should be resolved even if the line corresponding to the NH (ND) transition $b^1\Sigma^+$, v′ =

DOI: 10.1021/acs.jpca.7b09661
J. Phys. Chem. A 2017, 121, 9045−9057

$0 \rightarrow a^1\Delta^+$, $v'' = 0$, which was observed in an Ar matrix at λ = 1173.58 nm (1170.47 nm), is present in the spectra.[35]

Experiments with registration of lines from the samples in the near-IR region should resolve this problem. At the present time we do not have equipment to investigate emission in this (1100−1200 nm) wavelength range. We plan to perform these experiments in the future. We can conclude that, for the identification of the emission at λ = 473 nm, there are two possible candidates, the ND radical (transition $b^1\Sigma^+, v' = 0 \rightarrow X^3\Sigma^-$, $v'' = 0$) or the N^- anion (transition $^1S_0 \rightarrow {}^3P_1$). Both of these candidates have the same precursor $N(^2P)$ atom.

From the comparison of the observed bands at λ = 336 nm with the results of emission from $ND(A^3\Pi_i v' = 0 \rightarrow X^3\Sigma^-, v'' = 0)$ obtained in rare-gas matrices (see Table 7) we can assign this emission to the $A^3\Pi_i \rightarrow X^3\Sigma^-$ transition of the ND radical. The $A^3\Pi_i$-state of the ND radical is the result of the recombination of $N(^2D)$ and $D(^2S)$ atoms. Indeed we observed a correlation between intensities of emissions at λ = 336 nm and that of the α-group of N atoms, which supports the assignment for this emission.

Another candidate for emission of the band at 336 nm might be the N_2 molecule transition $C^3\Pi_g, v' = 0 \rightarrow B^3\Pi_g, v'' = 0$. In the gas phase this band is located at λ = 337 nm,[32] but there is no evidence for observation of this band in solid nitrogen.

The most interesting result obtained in this work is the observation of the rather intense broad band with the maximum at λ = 360 nm for hydrogen−nitrogen-helium and deuterium−nitrogen−helium samples. After analysis of our previous results we found that we observed only very weak bands at 360 nm during the destruction of nitrogen nanoclusters containing only stabilized nitrogen atoms and small (1×10^{-3} to 1×10^{-4}) admixtures of oxygen atoms.[13,16] The addition of H_2 or D_2 molecules in the gas mixture used for sample preparation resulted in a large enhancement of the intensity of the band appearing at λ = 360 nm in the luminescence spectra in the final stage of sample destruction (see Figures 4, 7, and 9). We found that the maximum intensity of the 360 nm band corresponds to some optimum quantity of H_2 or D_2 present in the makeup gas mixture. An important observation is that the addition of rare gases in the makeup gas mixture does NOT influence significantly the position of this band (see Figure 9).

In the literature there are two explanations for the emission bands at λ = 360 nm. The first observation of this broad band was obtained when solid nitrogen was irradiated by 400 eV electrons, and the band was assigned to an unidentified impurity.[67] Later this luminescence band was studied during the excitation of solid nitrogen films by 500 eV electrons.[32] The band was assigned to the emission of polynitrogen N_4^*, which was formed as a result of a neutralization reaction of N_4^+ with electrons in solid nitrogen. The scenario of "hole self-trapping" for N_2^+ ions with the formation of N_4^+ in a nitrogen matrix was quite recently proposed[23,68] because of the localized character of positive charge carriers in solid N_2.[69] This suggestion is in good accordance with both the study of gas-phase equilibria of solvation reactions of N_2^+ with N_2 molecules, which revealed electrostatic bonding in the core clusters N_4^+[70] and the laser-induced dissociation experiments showing N_4^+ as the ionic core for the even ion clusters $N_2^+-(N_2)_n$.[71]

Another interpretation of the 360 nm band corresponding to the transition ND ($A^3\Pi$, $v' = 0 \rightarrow X^3\Sigma^-$, $v'' = 1$) was suggested from the analysis of the luminescence spectra of the 0.1% N_2-doped solid deuterium irradiated by electrons.[72] Emission of NH (ND) radicals was also studied in different solid rare gases. It was found that the position of the (0−1) $NH(A^3\Pi \rightarrow X^3\Sigma^-)$ transition is shifted by a few nanometers for different solid rare gases and that the band had a resolved structure.[41] We rule out this interpretation because of the unusual broad shape of the observed band at λ = 360 nm and the absence of the more intense emission of the (0−0) $NH(A^3\Pi \rightarrow X^3\Sigma^-)$ transition.

In our experiments the spectra of the 360 nm band were not significantly influenced by the addition of rare gases or by the replacement of hydrogen isotopes in the nitrogen nanoclusters. This would also give a preference for the interpretation of the observed band at 360 nm in our experiments as an emission of N_4 polynitrogen. However, the question remains open as to why this emission was enhanced when the impurities of H_2 or D_2 were present in the molecular nitrogen nanoclusters. A possible explanation of this behavior is the change of the efficiency of formation of N atoms in the discharge zone with the addition of H_2 and D_2 molecules. It has been known for many years that the presence of water vapor in nitrogen discharges increases the production of N atoms via dissociation of N_2 molecules.[17]

For the conditions of our experiments, the formation mechanism of N_4 polynitrogen predicted in earlier theoretical work[33] can be realized. It was shown that the barrier for N_4 compound formation from two nitrogen molecules in the excited metastable $A^3\Sigma_u^+$ states is very small (~0.25 eV).[33] Intense recombination of $N(^4S)$ atoms during the explosive destruction of the samples results in high concentrations of metastable $N_2(A^3\Sigma_u^+)$ molecules[16] that can participate in bimolecular reactions to form N_4 compounds. The potential curves for different electronic configurations of $N_4(D_{2h})$ polynitrogen is shown in Figure 12. The bound state of the

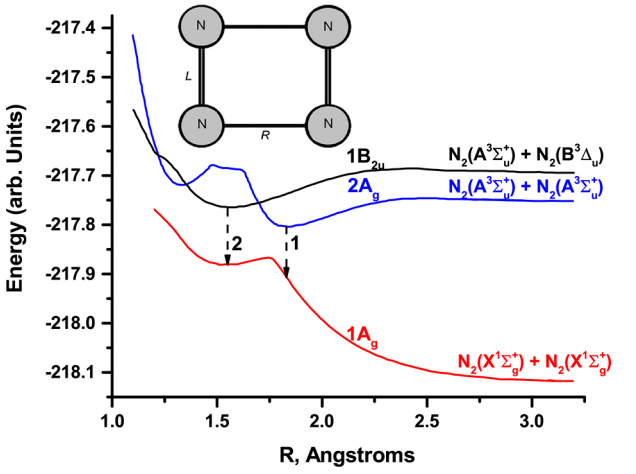

Figure 12. Dependence of the system energy on the distance R between N_2 molecules. Each curve corresponds to the indicated symmetry of the wave function. The interatomic distance inside the N_2 molecule was L = 1.274 Å. (inset) An N_4 cluster of D_{2h} symmetry.[33]

N_4 compound in the potential curve of two interacting triplet molecules is located at a distance R = 1.83 Å between molecules (see Figure 12). The lower potential curve of the N_4 compound for the interaction of two N_2 molecules in the ground state at this distance has a repulsive character (see red curve in Figure 12). Therefore, the emission from the bound triplet−triplet $2A_g$ state of N_4 to the singlet−singlet $1A_g$ state involving the dissociation of the compound into two molecules (transition 1 in Figure 12) should be broad and without any structure just as

DOI: 10.1021/acs.jpca.7b09661
J. Phys. Chem. A 2017, 121, 9045−9057

for the case of excimer molecules. The predicted energy of the emitted quantum is ~3.1 eV. Both of these predictions are in good agreement with the broad nonstructured emission with a maximum at λ = 360 nm ($E \approx 3.44$ eV) observed in our experiments. According to this analysis we can thus assign the observed emission at $\lambda \approx 360$ nm to the $2A_g \rightarrow 1A_g$ transition of the $N_4(D_{2h})$ compound.[33] After emission the compound dissociates into two N_2 molecules in the ground state.

In the case of formation of N_4 compounds as a result of the interaction of $N_2(A^3\Sigma_u^+)$ and $N_2(B^3\Delta_u)$, the potential curve has a minimum at R = 1.55 Å. At this distance there is also a minimum in the potential curve of N_4 resulting from the interaction of two N_2 $(X^1\Sigma_g^+)$ molecules in the ground state (see Figure 12). This means that after emission of the quantum with energy of ~3 eV (transition 2 in Figure 12) the N_4 compound will remain in the metastable state providing possibility for the formation of an HEDM. Further experimental and theoretical work would be desirable to realize HEDMs from N_4 polynitrogen.

CONCLUSIONS

1. The process of stabilizing high concentrations of ground-state atoms in molecular nitrogen nanoclusters provides a unique opportunity to study low-temperature reactions and to produce a variety of unusual species in excited states.
2. A weak broad band at 360 nm is observed during the destruction of ensembles of molecular nitrogen nanoclusters containing stabilized nitrogen and small admixtures of oxygen atoms. This band was greatly enhanced in the spectra of samples prepared from gas mixtures that contained hydrogen or deuterium.
3. Since this band is not changed significantly in rare-gas matrices, we suggest that N_4^* polynitrogen molecule is responsible for the emission of the band at 360 nm. The exact shape and location of the 360 nm band is not altered by hydrogen isotope substitution. These N_4 polynitrogen compounds are formed during the process of sample destruction accompanied by fast chemical reactions of nitrogen atoms and molecules.
4. The observed emission at $\lambda \sim 336$ nm was assigned to the ND radical, $A^3\Pi$, $v' = 0 \rightarrow X^3\Sigma$, $v'' = 0$ transition.
5. The observed emission at λ = 473 nm may be assigned to the ND radical, $b^1\Sigma^+$, $v' = 0 \rightarrow X^3\Sigma^-$, $v'' = 0$ transition, but the alternative assignment to the N^- anion $^1S_0 \rightarrow {}^3P_1$ transition, can also be considered.

AUTHOR INFORMATION

Corresponding Author

*E-mail: khmel@physics.tamu.edu.

ORCID

Vladimir V. Khmelenko: 0000-0002-3362-3891

Notes

The authors declare no competing financial interest.

ACKNOWLEDGMENTS

This work was supported by NSF Grant No. DMR 1707565.

REFERENCES

(1) Clark, R. N.; Carlson, R.; Grundy, W.; Noll, K. In *The Science of Solar System Ices,* 1st ed.; Gudipati, M. S., Castillo-Rogez, J., Eds.; Astrophysics and Space Science Library; Springer: New York, 2013; Vol. *356*, pp 3–46.

(2) Khmelenko, V. V.; Kunttu, H.; Lee, D. M. Recent Progress in Studies of Nanostructured Impurity-Helium Solids. *J. Low Temp. Phys.* **2007**, *148*, 1–31.

(3) Boltnev, R. E.; Krushinskaya, I. N.; Pelmenev, A. A.; Popov, E. A.; Stolyarov, D. Y.; Khmelenko, V. V. Study of The Stabilization and Recombination of Nitrogen Atoms in Impurity-Helium Condensates. *Low Temp. Phys.* **2005**, *31*, 547–555.

(4) Bernard, E. P.; Boltnev, R. E.; Khmelenko, V. V.; Lee, D. M. Stabilization of High Concentrations of Nitrogen Atoms in Impurity-Helium Solids. *J. Low Temp. Phys.* **2004**, *134*, 199–204.

(5) Mao, S.; Boltnev, R. E.; Khmelenko, V. V.; Lee, D. M. ESR Studies of Nitrogen Atoms Stabilized in Aggregates of Krypton-Nitrogen Nanoclusters Immersed in Superfluid Helium. *Low Temp. Phys.* **2012**, *38*, 1037–1042.

(6) Gordon, E. B.; Mezhov-Deglin, L. P.; Pugachev, O. F. Stabilization of Nitrogen Atoms in Superfluid Helium. *J. Exp. Theor. Phys. Lett.* **1974**, *19*, 63–65.

(7) Gordon, E. B.; Mezhov-Deglin, L. P.; Pugachev, O. F.; Khmelenko, V. V. Condensation of an Atomic Beam on a Cold (⩽2 K Surface). *Cryogenics* **1976**, *16* (9), 555–557.

(8) Gordon, E. B.; Pelmenev, A. A.; Pugachev, O. F.; Khmelenko, V. V. Hydrogen and Deuterium Atoms, Stabilized by Condensation of an Atomic Beam in Superfluid Helium. *J. Exp. Theor. Phys. Lett.* **1983**, *37*, 237–239.

(9) Kiselev, S. I.; Khmelenko, V. V.; Lee, D. M. Hydrogen Atoms in Impurity-Helium Solids. *Phys. Rev. Lett.* **2002**, *89*, 175301.

(10) Khmelenko, V. V.; Bernard, E. P.; Vasiliev, S.; Lee, D. M. Tunnelling Chemical Reactions of Hydrogen Isotopes in Quantum Solids. *Russ. Chem. Rev.* **2007**, *76*, 1107–1121.

(11) Mao, S.; Meraki, A.; Boltnev, R. E.; Khmelenko, V. V.; Lee, D. M. Percolation in Aggregates of Nanoclusters Immersed in Superfluid Helium. *Phys. Rev. B: Condens. Matter Mater. Phys.* **2014**, *89*, 144301.

(12) Boltnev, R. E.; Krushinskaya, I. N.; Pelmenev, A. A.; Stolyarov, D. Y.; Khmelenko, V. V. The Thermoluminescence Spectra Obtained on the Destruction of Impurity-Helium Solid Phase Samples. *Chem. Phys. Lett.* **1999**, *305*, 217–224.

(13) Khmelenko, V. V.; Lee, D. M.; Krushinskaya, I. N.; Boltnev, R. E.; Bykhalo, I. B.; Pelmenev, A. A. Dynamics of Thermoluminescence Spectra of Impurity-Helium Condensates Containing Stabilized Nitrogen and Oxygen Atoms. *Low Temp. Phys.* **2012**, *38*, 688–699.

(14) Khmelenko, V. V.; Pelmenev, A. A.; Krushinskaya, I. N.; Bykhalo, I. B.; Boltnev, R. E.; Lee, D. M. Energy Release Channels During Destruction of Impurity-Helium Condensates. *J. Low Temp. Phys.* **2013**, *171*, 302–308.

(15) Boltnev, R. E.; Bykhalo, I. B.; Krushinskaya, I. N.; Pelmenev, A. A.; Khmelenko, V. V.; Mao, S.; Meraki, A.; Wilde, S. C.; McColgan, P. T.; Lee, D. M. Optical and Electron Spin Resonance Studies of Xenon-Nitrogen-Helium Condensates Containing Nitrogen and Oxygen Atoms. *J. Phys. Chem. A* **2015**, *119*, 2438–2448. PMID: 25353614.

(16) Meraki, A.; Mao, S.; McColgan, P. T.; Boltnev, R. E.; Lee, D. M.; Khmelenko, V. V. Thermoluminescence Dynamics During Destructions of Porous Structures Formed by Nitrogen Nanoclusters in Bulk Superfluid Helium. *J. Low Temp. Phys.* **2016**, *185*, 269–286.

(17) Bass, A. M.; Broida, H. P. Spectra Emitted from Solid Nitrogen Condensed at 4.2 K from a Gas Discharge. *Phys. Rev.* **1956**, *101*, 1740–1747.

(18) Samartzis, P. C.; Wodtke, A. M. All-Nitrogen Chemistry: How Far Are We From N_{60}? *Int. Rev. Phys. Chem.* **2006**, *25*, 527–552.

(19) Douglas, A.; Jones, W. J. The 2700Å Bands of the N_3 Molecules. *Can. J. Phys.* **1965**, *43*, 2216–2221.

(20) Tian, R.; Michl, J. Fast-Particle Bombardment of Solid Nitrogen. *Faraday Discuss. Chem. Soc.* **1988**, *86*, 113–124.

(21) Amicangelo, J. C.; Collier, J. R.; Dine, C. T.; Saxton, N. L.; Schleicher, R. M. Matrix Isolation Infrared Observation of N_3 Using a Nitrogen Microwave Discharge Plasma Source. *Mol. Phys.* **2007**, *105*, 989–1002.

DOI: 10.1021/acs.jpca.7b09661
J. Phys. Chem. A 2017, 121, 9045–9057

(22) Wu, Y.-J.; Chen, H.-F.; Chuang, S.-J.; Huang, T.-P. Far Ultraviolet Absorption Spectra of N_3 and N_2^+ Generated by Electrons Impacting Gaseous N_2. *Astrophys. J.* **2013**, *779*, 40−46.
(23) Savchenko, E. V.; Khyzhniy, I. V.; Uyutnov, S. A.; Barabashov, A. P.; Gumenchuk, G. B.; Beyer, M. K.; Ponomaryov, A. N.; Bondybey, V. E. Radiation Effects in Solid Nitrogen and Nitrogen-Containing Matrices: Fingerprints of N_4^+ Species. *J. Phys. Chem. A* **2015**, *119*, 2475−2482.
(24) Savchenko, E.; Khyzhniy, I.; Uyutnov, S.; Bludov, M.; Gumenchuk, G.; Bondybey, V. Emission Spectroscopy of Solid Nitrogen. *Radiat. Meas.* **2016**, *90*, 1−5. Proceedings of the ninth International Conference on Luminescent Detectors and Transformers of Ionizing Radiation (LUMDETR 2015).
(25) Christe, K. O.; Wilson, W. W.; Sheehy, J. A.; Boatz, J. A. N_5^+: A Novel Homoleptic Polynitrogen Ion as a High Energy Density Material. *Angew. Chem., Int. Ed.* **1999**, *38*, 2004−2009.
(26) Vij, A.; Wilson, W. W.; Vij, V.; Tham, F. S.; Sheehy, J. A.; Christe, K. O. Polynitrogen Chemistry. Synthesis, Characterization, and Crystal Structure of Surprisingly Stable Fluoroantimonate Salts of N_5^+. *J. Am. Chem. Soc.* **2001**, *123*, 6308−6313. PMID: 11427055.
(27) Nguyen, M. T. Polynitrogen compounds: 1. Structure and Stability of N_4 and N_5 Systems. *Coord. Chem. Rev.* **2003**, *244*, 93−113. 13th Main Group Chemistry.
(28) Zarko, V. E. Searching For Ways to Create Energetic Materials Based on Polynitrogen Compounds (review). *Combust., Explos. Shock Waves* **2010**, *46*, 121−131.
(29) Cacace, F.; de Petris, G.; Troiani, A. Experimental Detection of Tetranitrogen. *Science* **2002**, *295*, 480−481.
(30) Rennie, E. E.; Mayer, P. M. Confirmation of the "Long-Lived" Tetra-Nitrogen (N_4) Molecule Using Neutralization-Reionization Mass Spectrometry and ab initio Calculations. *J. Chem. Phys.* **2004**, *120*, 10561−10578.
(31) Zheng, J. P.; Waluk, J.; Spanget-Larsen, J.; Blake, D. M.; Radziszewski, J. Tetrazete (N_4). Can it be Prepared and Observed? *Chem. Phys. Lett.* **2000**, *328*, 227−233.
(32) Savchenko, E. V.; Khyzhniy, I. V.; Uyutnov, S. A.; Bludov, M. A.; Barabashov, A. P.; Gumenchuk, G. B.; Bondybey, V. E. Radiation Effects in Solid Nitrogen. *J. Low Temp. Phys.* **2017**, *187*, 62−70.
(33) Elesin, V. F.; Degtyarenko, N. N.; Pazhitnykh, K. S.; Matveev, N. V. Modeling of Synthesis and Dissociation of the N_4 Nitrogen Cluster of D_{2H} Symmetry. *Russ. Phys. J.* **2009**, *52*, 1224−1234.
(34) Graham, W. R. M.; Lew, H. Spectra of the $d^1\Sigma^+ - c^1\Pi$ and $d^1\Sigma^+ - b^1\Sigma^+$ Systems and Dissociation Energy of NH and ND. *Can. J. Phys.* **1978**, *56*, 85−99.
(35) Ramsthaler-Sommer, A.; Becker, A. C.; Van Riesenbeck, N.; Lodemann, K.-P.; Schurath, U. Branching Ratios and Radiative Rates of Matrix-Isolated NH in Argon: The $b^1\Sigma^+ \rightarrow a^1\Delta$, $X^3\Sigma^-$ and $a^1\Delta \rightarrow X^3\Sigma^-$ Transitions. *Chem. Phys.* **1990**, *140*, 331−338.
(36) Robinson, G. W.; McCarty, M., Jr. Electronic Spectra of Free Radicals at 4 K-HNO, NH, and OH. *J. Chem. Phys.* **1958**, *28*, 350.
(37) McCarty, M., Jr; Robinson, G. W. Imine and Imine-d Radicals Trapped in Argon, Krypton and Xenon Matrices at 4.2 K. *J. Am. Chem. Soc.* **1959**, *81*, 4472−4476.
(38) Lund, P. A.; Hasan, Z.; Schatz, P. N.; Miller, J. H.; Andrews, L. Matrix Isolation Magnetic Circular Dichroism (MCD) Spectrum of NH Radical Produced by a Glow Discharge Technique. *Chem. Phys. Lett.* **1982**, *91*, 437−439.
(39) Schnepp, O.; Dressler, K. Photolysis of Ammonia in a Solid Matrix at Low Temperatures. *J. Chem. Phys.* **1960**, *32*, 1682−1686.
(40) Van De Bult, C. E. P. M.; Allamandola, L. J.; Baas, F.; Van Ijzenboorn, L.; Greenberg, J. M. Chemiluminescence of N_2, NH, and O_2 in Argon Matrices. *J. Mol. Struct.* **1980**, *61*, 235−238.
(41) Bondybey, V. E.; Brus, L. E. Interdependence of Guest Radiationless Transitions and Localized Phonon Structure: NH and ND($A^3\Pi$) in Rare Gas Lattices. *J. Chem. Phys.* **1975**, *63*, 794−804.
(42) Goodman, J.; Brus, L. E. Long Range Vibrational Energy Transfer from ND and NH($A^3\Pi$) to CO and N_2 in Solid Ar. *J. Chem. Phys.* **1976**, *65*, 1156−1164.
(43) Bondybey, V. E.; English, J. H. Effect of Matrix on Vibrational Relaxation: NH and ND $X^3\Sigma^-$ in Rare Gas Solids. *J. Chem. Phys.* **1980**, *73*, 87−92.
(44) Ramsay, D. A.; Sarre, P. J. The $c^1\Pi - a^1\Delta$ System of the NH Molecule. *J. Mol. Spectrosc.* **1982**, *93*, 445−446.
(45) Cheung, W. Y.; Gelernt, B.; Carrington, T. New Bands in the ND $c^1\Pi - a^1\Delta$ System: Spectroscopic Constants of the $a^1\Delta$ State. *Chem. Phys. Lett.* **1979**, *66*, 287−290.
(46) Lunt, R. W.; Pearse, R. W. B.; Smith, E. C. W. The λ 4502 Band of NH. *Proc. R. Soc. London, Ser. A* **1935**, *151*, 602−609.
(47) Whittaker, F. L. The $c^1\Pi - b^1\Sigma^+$ Band System of NH and ND. *J. Phys. B: At. Mol. Phys.* **1968**, *1*, 977−982.
(48) Whittaker, F. L. Observation of the $d^1\Sigma - b^1\Sigma^+$ System of NH and ND in The Vacuum Ultraviolet. *Can. J. Phys.* **1969**, *47*, 1291−1293.
(49) Esser, H.; Langen, J.; Schurath, U. Spectrum and Lifetime of NH($a^1\Delta \rightarrow X^3\Sigma^-$) in Inert Gas Matrices. *Berichte der Bunsengesellschaft für physikalische Chemie* **1983**, *87*, 636−643.
(50) Hizhnyakov, V.; Seranski, K.; Schurath, U. Homogeneous Lineshapes and Shifts of The $b^1\Sigma^+ \leftarrow X^3\Sigma^-$ Transition in Matrix-Isolated NH: Comparison With Quadratic Coupling Theory. *Chem. Phys.* **1992**, *162*, 249−256.
(51) Boltnev, R. E.; Bykhalo, I. B.; Krushinskaya, I. N.; Pelmenev, A. A.; Mao, S.; Meraki, A.; McColgan, P. T.; Lee, D. M.; Khmelenko, V. V. Spectroscopic Observation of Nitrogen Anions N^- in Solid Matrices. *Phys. Chem. Chem. Phys.* **2016**, *18*, 16013−16020.
(52) Oehler, O.; Smith, D. A.; Dressler, K. Luminescence Spectra of Solid Nitrogen Excited by Electron Impact. *J. Chem. Phys.* **1977**, *66*, 2097−2107.
(53) Coletti, F.; Bonnot, A. M. Emission Spectrum of Electron Excited Solid Nitrogen. *Chem. Phys. Lett.* **1977**, *45*, 580−582.
(54) Peyron, M.; Broida, H. P. Spectra Emitted from Solid Nitrogen Condensed at Very Low Temperatures from a Gas Discharge. *J. Chem. Phys.* **1959**, *30*, 139−150.
(55) Chergui, M.; Schwentner, N.; Tramer, A. Spectroscopy of The NO Molecule in N_2 and Mixed N_2/Kr Matrices. *Chem. Phys. Lett.* **1993**, *201*, 187−193.
(56) Kiryukhin, V.; Keimer, B.; Boltnev, R. E.; Khmelenko, V. V.; Gordon, E. B. Inert-Gas Solids with Nanoscale Porosity. *Phys. Rev. Lett.* **1997**, *79*, 1774−1777.
(57) Kiselev, S. I.; Khmelenko, V. V.; Lee, D. M.; Kiryukhin, V.; Boltnev, R. E.; Gordon, E. B.; Keimer, B. Structural Studies of Impurity-Helium Solids. *Phys. Rev. B: Condens. Matter Mater. Phys.* **2001**, *65*, 024517.
(58) Bernard, E. P.; Boltnev, R. E.; Khmelenko, V. V.; Kiryukhin, V.; Kiselev, S. I.; Lee, D. M. ESR and X-ray Investigations of Deuterium Atoms and Molecules in Impurity-Helium Solids. *J. Low Temp. Phys.* **2004**, *134*, 169−174.
(59) Bernard, E. P.; Boltnev, R. E.; Khmelenko, V. V.; Kiryukhin, V.; Kiselev, S. I.; Lee, D. M. Deuterium Atoms and Molecules in Nanoclusters of Molecular Deuterium. *Phys. Rev. B: Condens. Matter Mater. Phys.* **2004**, *69*, 104201.
(60) Kiryukhin, V.; Bernard, E. P.; Khmelenko, V. V.; Boltnev, R. E.; Krainyukova, N. V.; Lee, D. M. Noble-Gas Nanoclusters with Fivefold Symmetry Stabilized in Superfluid Helium. *Phys. Rev. Lett.* **2007**, *98*, 195506.
(61) Krainyukova, N. V.; Boltnev, R. E.; Bernard, E. P.; Khmelenko, V. V.; Lee, D. M.; Kiryukhin, V. Observation of the fcc-to-hcp Transition in Ensembles of Argon Nanoclusters. *Phys. Rev. Lett.* **2012**, *109*, 245505.
(62) Kiselev, S. I.; Khmelenko, V. V.; Lee, D. M. Sound Propagation in Liquid He in Impurity-Helium Solids. *Low Temp. Phys.* **2000**, *26*, 641−648.
(63) Kiselev, S. I.; Khmelenko, V. V.; Lee, D. M. Investigation of Ultrasound Attenuation in Impurity-Helium Solids Containing Liquid Helium. *J. Low Temp. Phys.* **2000**, *121*, 671−676.
(64) Bernard, E. P.; Khmelenko, V. V.; Lee, D. M. Pulse Electron Spin Resonance Studies of H and D Atoms in Impurity-Helium Solids. *J. Low Temp. Phys.* **2008**, *150*, 516−524.

DOI: 10.1021/acs.jpca.7b09661
J. Phys. Chem. A 2017, 121, 9045−9057

(65) Boltnev, R. E.; Bernard, E. P.; Järvinen, J.; Khmelenko, V. V.; Lee, D. M. Stabilization of Hydrogen Atoms in Aggregates of Krypton Nanoclusters Immersed in Superfluid Helium. *Phys. Rev. B: Condens. Matter Mater. Phys.* **2009**, *79*, 180506.
(66) Hack, W.; Haubold, R.; Heinrich-Sterzel, C.; Keller-Rudek, H.; Ohms, U.; Schiöberg, D.; Strametz, C. Compounds with Noble Gases and Hydrogen. In *Gmelin Handbook of Inorganic and Organometallic Chemistry*, 8th ed.; Springer-Verlag: Berlin, Germany, 1993; Vol. *N/0-b/b/1*.
(67) Fugol, I. Y.; Poltoratski, Y. B.; Rybalko, Y. I. Self-Localization of High-Frequency Triplet Excitations in Solid Nitrogen. *Low Temp. Phys.* **1978**, *4*, 1048−1052.
(68) Savchenko, E.; Khyzhniy, I.; Uyutnov, S.; Barabashov, A.; Gumenchuk, G.; Ponomaryov, A.; Bondybey, V. Charged Defects and Defect-Induced Processes in Nitrogen Films. *Phys. Status Solidi C* **2015**, *12*, 49−54.
(69) Loveland, R. J.; Le Comber, P. G.; Spear, W. E. Charge Transport in the Diatomic Molecular Solids and Liquids: N_2, O_2, and CO. *Phys. Rev. B* **1972**, *6*, 3121−3127.
(70) Hiraoka, K.; Nakajima, G. A Determination of the Stabilities of $N_2^+(N_2)_n$ and $O_2^+(N_2)_n$ with $n = 1 - 11$ From Measurements of the Gas-Phase Ion Equilibria. *J. Chem. Phys.* **1988**, *88*, 7709−7714.
(71) David, D. E.; Magnera, T. F.; Tian, R.; Stulik, D.; Michl, J. Cluster ions from keV-energy ion and atom bombardment of frozen gases. *Nucl. Instrum. Methods Phys. Res., Sect. B* **1986**, *14*, 378−391.
(72) Stenum, B.; Schou, J.; Sørensen, H.; Gürtler, P. Luminescence From Pure and Doped Solid Deuterium Irradiated by keV Electrons. *J. Chem. Phys.* **1993**, *98*, 126−134.

DOI: 10.1021/acs.jpca.7b09661
J. Phys. Chem. A 2017, 121, 9045−9057